

Observation of Asymmetric Sheath Structure in Multi-Component Plasma Containing Negative Ions

KOGA Kazunori, NAITOU Hiroshi¹ and KAWAI Yoshinobu
*Interdis. Grad. School of Eng. Sci., Kyushu University,
6-1 Kasuga-kouen, Kasuga, Fukuoka 816-8580, Japan*
¹*Faculty of Engineering, Yamaguchi University
Tokiwadai 2557, Ube, Yamaguchi 755-8611, Japan*

(Received: 11 December 1998 / Accepted: 9 May 1999)

Abstract

The formation of the asymmetric sheath formed around the separation grid of a Double Plasma machine was experimentally investigated in a negative ion plasma in order to clarify the physical mechanism of the ion sheath instability. It was found that cluster ions are produced in the ion sheath and play an important role in the excitation of the ion sheath instability. Furthermore, the suppression of the ion sheath instability by the introduction of negative ions is discussed.

Keywords:

asymmetric ion sheath, negative ion, ion sheath instability

1. Introduction

The ion sheath instability caused by an asymmetry of the ion sheath formed around the separation grid of a Double Plasma (D.P.) machine is of interest from the viewpoint of nonlinear dynamics in plasma [1-3]. The asymmetry of the ion sheath is realized by the plasma density or the space potential difference between two plasma regions which is divided by a separation mesh grid. Recently, the behavior of this sheath in a two-component plasma was discussed experimentally and numerically [4]. It was pointed out that the group behavior of ions in the sheath and presheath regions plays an important role in the excitation of the instability and that oscillation of the plasma potential and the ion bounce motion inside the ion sheath produce cluster ions, leading to the ion sheath instability. However, it is hard to investigate detailed structures of the ion sheath since the methods of the measurement are restricted. It has been pointed out that there are a lot of negative ions in various plasmas. When negative ions

exist, the ion sheath instability is influenced by negative ions: increasing the negative ion concentration α , the sheath width becomes large, as predicted from the Child-Langmuir equation. Thus, it is expected that the investigation of the ion sheath instability in a negative ion plasma is useful for understanding the physical mechanism of the ion sheath instability. Recently, we succeeded in observing the ion sheath instability in a negative ion plasma [5]. The ion sheath instability is excited for certain grid bias potential. When the α was increased, the ion sheath instability was suppressed.

In this work, we studied, in detail, the sheath structures in a negative ion plasma in order to clarify the physical mechanism for the excitation of the ion sheath instability and one model is presented. Furthermore, the suppression of the ion sheath instability by the introduction of negative ions is discussed based on the experimental results and numerical simulations.

Corresponding author's e-mail: koga@ed.kyushu-u.ac.jp

2. Experimental Apparatus

The experiments were carried out with a D.P. machine whose diameter and length are 50cm and 100cm, respectively. In this experiment, we made use of the Ar and SF₆ gases. Negative ions were generated by electron attachment on SF₆ and, as a result, a multi-component plasma was formed. The separation grid was located at the center of the D.P. machine in order to divide into two plasma regions (Driver and Target region). Plasma parameters were measured with a 6 mm diam. plain Langmuir probe. The axial profiles of the space potential and the ion saturation current were measured with an emissive probe and a Langmuir probe, respectively. In the target region, the electron temperature and plasma density was 0.5–1.0eV and $(1 - 10) \times 10^8 \text{cm}^{-3}$, respectively. In the driver region, the plasma density was below one tenth of that. The separation grid was biased at potential V_g . Fluctuating parts of the separation grid current were obtained from the voltage drop across the resistor and were analyzed with a spectrum analyzer. The negative ion concentration α was estimated by $\alpha = 1 - I'_{es}/I_{es}$, where the I_{es} is the electron saturation current in the

argon plasma which obtained from the probe characteristic and the I'_{es} is the negative current in the negative ion plasma. The mass of the negative ion is much heavier than that of the electron so that if α is not very high, the probe current of the negative ion becomes negligibly small compared with the electron saturation current until the high α . Therefore, this estimation gives a correct concentration.

3. Results and Discussion

When the electron density of the target region in the D.P. machine was higher than that of the driver region and the separation grid was biased negatively, a fluctuation with a sharp peak frequency was observed in the grid current, that is, the ion sheath instability is excited. We investigated the sheath structure under this situation. The grid bias was kept constant at $|V_g| = 100\text{V}$ (with the instability). Figure 1 shows typical time-averaged axial profiles of the sheath potential and the ion saturation current (I_{is}) for various α . When α is increased, the space potential of the bulk plasma tends to decrease. This tendency is stronger in the driver region. The space potential drops from about 2.6V to 2.1V in the target region and from about 6V to 5V in the driver region. Thus, the fluctuation becomes harder to be excited because the negative ions decrease the space potential especially in the driver region. Figure 1 also indicates that a potential swell appears near the sheath edge in the driver (low density) region. Local structures in the I_{is} profiles are formed near the sheath edge at both target and driver sides.

In order to investigate the formation of the sheath structures, we carried out a simulation with the one-dimensional particle-in-cell code that treats the two-components (electron and proton) plasma. In this simulation, we adopted the same simulation parameters which were used in Ref. 1. Figure 2 shows the time-averaged profiles of the potential and the ion density. Here, these profiles were time-averaged by taking the snap shots. Total sampling time corresponds to about $9.34\omega_{pi}^{-1}$. The electron density in the target and driver region settled down about 147 and 14 (particles/simulation mesh), respectively. It was found that the density difference of about one order exists at this time. Here, the grid potential was kept constant at $\phi_g (\equiv \frac{eV_g}{T_e}) = -200$. Three peaks (P1, P2 and P3) were observed in the ion density profile. Figure 2(b) shows an enlargement graph of Fig. 2(a) in the target region. There is no local potential structure such as the swell in the target region. Figure 2(c) shows the time-averaged profile in the driver

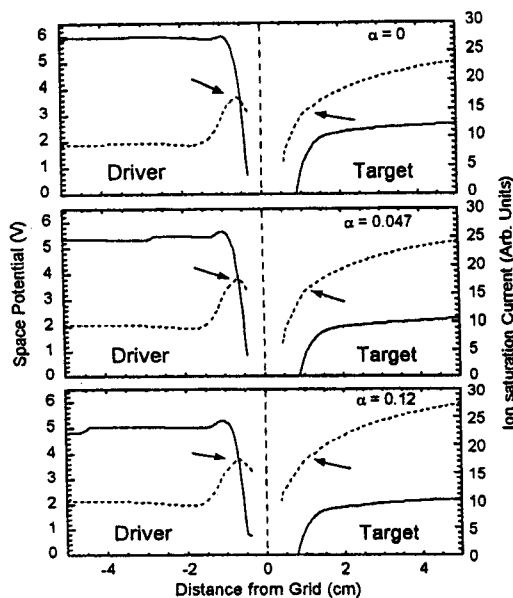


Fig. 1 The axial profiles of the space potential and the ion saturation current (I_{is}) around the separation grid for various α . The grid bias was kept at $|V_g| = 100\text{V}$ (with the fluctuation). Here, the solid lines, the broken lines and the arrows indicate the potential profiles, the I_{is} profiles and the position of the local structures near the sheath edge, respectively.

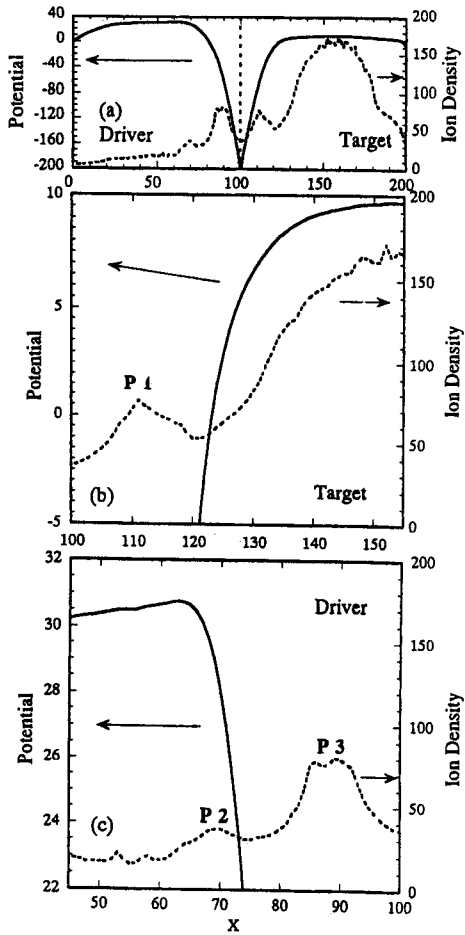


Fig. 2 Time-averaged profiles of the potential and the ion density in (a) the whole system, (b) the target region and (c) the driver region. Here, the solid line and broken line indicate the potential profile and the ion density profile, respectively.

region, indicating that the potential swell is formed near the sheath edge. As seen from these figures, these simulation results well reproduce the potential profile in the experiment. Simultaneously, the ion density peak P2 is formed near the potential swell.

It was also found that the space potential of the bulk plasma oscillates such as the potential relaxation in both target and driver regions in this simulation. Figure 3 shows the time evolution of the potential (first row of the graphs), ion density (second) and ion phase space (third) profiles. The density and the ion velocity are normalized to the initial density in the target region and the electron thermal velocity, respectively. In both target and driver regions, the ion density peak, which is formed inside the sheath, penetrates into the plasma region. The ions bounce inside the sheath as a cluster as shown in the phase space graphs. When the cluster of ions reaches the each sheath edge ($t = 55800$ and 56200), it was observed that the ion peak rush out to the plasma region. Ions are accumulated in the sheath region by the inflow of ions into the driver region from the target region and the ion bounce motion inside the sheath. The surplus ions inside sheath are pushed back to the separation grid by the increase of the ambipolar potential and the space potential increase in the driver region ($t = 55000$). The space potential is decreased by the potential relaxation ($t = 55800$) and oscillates. The space potential oscillates in the target region by the same process. However, the amplitude of the oscillation is very small, because the plasma density is high and is not so influenced. The time-averaged bulk potential is seen to be increased by the potential oscillation. Since

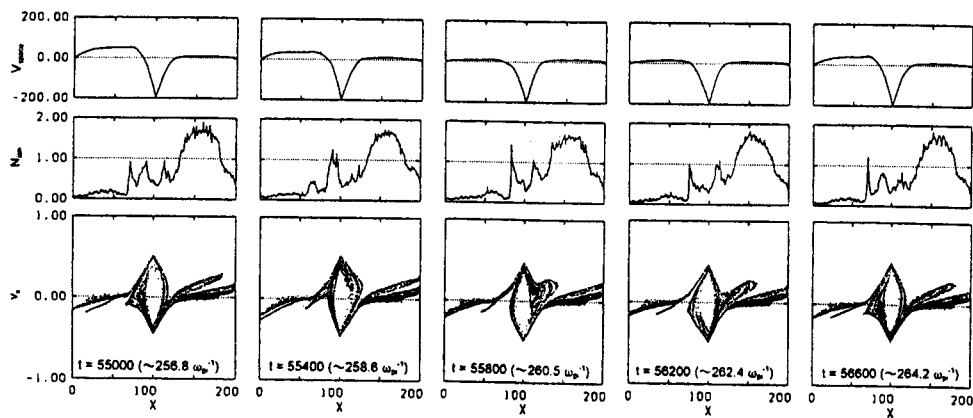


Fig. 3 Time evolution of the potential profiles (first row of graphs), the ion density profiles (second) and the ion phase space (third). These graphs are taken the snap shots from $t = 55000$ to $t = 56600$. The sampling time is 400 time steps which correspond to about $2 \omega_{pi}^{-1}$.

this behavior remarkably appears in the driver region, the time-averaged space potential of the bulk plasma in the driver region becomes larger than that in the target region. The ion density peak reflects near the sheath edge and penetrates into the plasma region in the simulation. The observed peak of the ion saturation current is appeared by such behavior of the ion density peak. Therefore, the large peak (arrows in Fig. 1) in I_{is} is larger than the ion density peak P2 (Fig. 2(c)). This result indicates that the reflection and penetration of ions occur at the location of the local structure in the I_{is} profile. Therefore, the reflection motion of the large ion flow forms the local structures of I_{is} near the sheath edge. The ion density peaks P1, P3 correspond to the ion cluster which bounces inside the sheath.

When the negative ion concentration α was increased, the time-averaged potential decreased in the bulk plasma region (Fig. 1). These results suggest that negative ions suppress the potential oscillations. As seen from Fig. 1, the peak height of the ion saturation current, which is formed near the sheath edge in the driver region, is independent of α . Negative ions are much heavier than the electron and remain in the presheath region. Since the total current is decreased by the negative ion in the presheath region, the power necessary for the oscillation to occur is loosed. That is, the suppression of the oscillation causes the decrease of the time-averaged potential and does not make synchronization between the potential oscillations and

the ion bounce oscillation. Thus, when α is increased, the ion sheath instability is suppressed.

4. Conclusions

The structure of the asymmetric ion sheath was investigated in a negative ion plasma. When the negative ion concentration was increased, the ion sheath instability was suppressed and the bulk potential tended to decrease. The tendency of the potential decrease was stronger in the driver region. In the PIC simulation, it was observed that the potential is oscillated by the ion bounce motion inside the sheath. It was considered that the potential oscillations are suppressed by the existence of negative ions in the presheath region. Then, the time-averaged potential is decreased. It is concluded from these results that the dumping of the potential oscillation by negative ions and the lack of the synchronism between the potential oscillations and the ion bounce oscillations suppress the ion sheath instability.

References

- [1] N. Ohno *et al.*, Phys. Fluids **B3**, 228 (1991).
- [2] G. Popa and R. Schrittwieser, Phys. Plasmas **1**, 32 (1994).
- [3] A. Piel *et al.*, Phys. Lett. **A216**, 296 (1996).
- [4] K. Koga *et al.*, J. Phys. Soc. Jpn. **68**, 1578 (1999).
- [5] K. Koga and Y. Kawai, Jpn. J. Appl. Phys. **38**, 1553 (1999).